

LASER BEAMS

PACS numbers: 42.60.Jf; 42.25.Gy; 42.79.Dj
DOI: 10.1070/QE2015v045n08ABEH015602

A wave model of refraction of laser beams with a discrete change in intensity in their cross section and their application for diagnostics of extended nonstationary phase objects

I.L. Raskovskaya

Abstract. **A beam model with a discrete change in the cross-sectional intensity is proposed to describe refraction of laser beams formed on the basis of diffractive optical elements. In calculating the wave field of the beams of this class under conditions of strong refraction, in contrast to the traditional asymptotics of geometric optics which assumes a transition to the infinite limits of integration and obtaining an analytical solution, it is proposed to calculate the integral in the vicinity of stationary points. This approach allows the development of a fast algorithm for correct calculation of the wave field of the laser beams that are employed in probing and diagnostics of extended optically inhomogeneous media. Examples of the algorithm application for diagnostics of extended nonstationary objects in liquid are presented.**

Keywords: *laser beam, optically inhomogeneous medium, refraction, wave field, laser diagnostics, physical processes in liquid.*

1. Introduction

In connection with the use of diffractive optical elements (DOEs) in laser technology [1], which possess a variety of opportunities for laser radiation conversion, the problem of studying the features of the wave fields of the beams formed by DOEs under different conditions of wave propagation is very urgent. Besides, of practical interest is the use of these beams as a probe in the reconstruction of spatial and temporal characteristics of physical processes resulting in an optical inhomogeneity of the medium [2]. Traditionally, the diagnostics of extended nonstationary phase objects employs fast angular scanning of laser beams; however, as indicated in [3], such a scanning is one of the most difficult problems of the control over the laser radiation characteristics. An alternative is the use of wide beams to ensure the probing of the entire region of interest. In this case, the transverse dimension W of the probing beam must be larger than the typical transverse dimension a of the gradient dynamic inhomogeneity or approximately equal to it.

In Fig. 1a an inhomogeneous layer in a density-stratified liquid is probed by a wide defocused laser beam [4], followed by a significant refraction, which leads to the formation of a caustic and multipath areas [5]. In this case, quantitative diagnostics of the inhomogeneity is complicated because of the complex nature of the refractive pattern. In such a situation the use of the beams formed by DOEs, which are visualised in the cross section as a matrix of points, a set of parallel segments, nested rings, etc. [6] allows using the offset of the beam structure elements as an informative parameter (Fig. 1b). This enables reconstructing the refraction index of an inhomogeneous structure using the methods of solving the inverse problem of refraction [7, 8]. We have described [7] the methods of the reconstruction of phase objects based on the ray representation of radiation propagation and registration of the offset of beam elements.

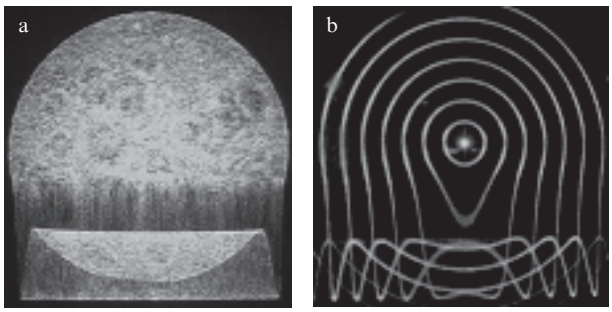

Figure 1. Experimental refractive images of the beam sections with (a) continuous and (b) discrete intensity variation.

However, under the conditions of strong refraction, with substantial 'blurring' of the beam elements and caustic formation, it is not always clear what should be meant under the element offset; therefore, solving the problem on diagnostics of medium parameters requires the use of additional information about the field intensity calculated on the basis of wave methods.

The problem that immediately arises in the wave field calculation is that the direct use of the parabolic equation and Kirchhoff integral for a sufficiently large cross-sectional area of the probe beam in the presence of strong refraction requires very significant computational resources, especially in the region of geometric optics, because of the necessity of integrating the rapidly oscillating functions. It should be noted that the calculation of the intensity on the basis of the traditional ray-optics asymptotics that requires a transition to the infinite limits of integration is impossible in the field of caustics.

In connection with the aforesaid, we propose here a 'fast' algorithm for calculating the refractive fields, which is valid in the field of caustics and allows real-time diagnostics of strongly inhomogeneous media.

I.L. Raskovskaya National Research University 'MPEI', Krasnokazarmennaya ul. 14, 111250 Moscow, Russia; e-mail: RaskovskaIL@mail.ru

Received 27 June 2014; revision received 12 February 2015
Kvantovaya Elektronika **45** (8) 765–770 (2015)
Translated by M.A. Monastyrskiy

To describe the radiation wave field formed by DOEs, it is advisable to use a model with a discrete change in beam intensity I over its section, for example, an annular beam model (Fig. 1b):

$$I(r) = \sum_{j=0}^{J} I_j \exp\left[-\frac{(r - j\Delta W)^2}{w_j^2}\right],$$

where r is the distance from the beam centre; $j = 0, \ldots, J$ is the number of the beam structure element (the ring number in the case under consideration); w_j and I_j are the characteristic size (width) and intensity of the ring with the number j; and ΔW is the spacing between the structure elements, which, in general, can be variable. The value of $W = J\Delta W$, i.e. the radius of the last ring, is considered as a characteristic size of the beam cross section. We assume that the condition $\Delta W \gg w_j$ is fulfilled for all j. Then we can approximately put the zero intensity everywhere, except the areas defined by the relation

$$j\Delta W - \delta_j \ll r \ll j\Delta W + \delta_j,$$

or, in other words, within each element with effective width δ_j, which in this case can be considered equal to $2w_j$.

This model turns out fruitful in the refractive field calculation, because it enables exclusion from integrating the areas with a zero intensity, which reduces the calculation time by several orders.

2. Asymptotic representation of the wave field in refraction of the beams with a discrete change in intensity over the cross section

To describe the coordinate- and time dependent wave field $A(x, y, z, t)$ that originally propagates along the z axis and passes through the optical inhomogeneity, we use the model of a transparent medium with a given refractive index $n = n(x, y, z, t)$ and boundaries $z = 0$ and $z = z_1$. Suppose that $A_0(x, y)$ is the complex amplitude of the beam at the entrance into the inhomogeneity region, λ is the laser radiation wavelength in free space and $k = 2\pi/\lambda$ is the wave number. Note that such a statement of the problem does not initially impose any restrictions on the behaviour of the field $A_0(x, y)$ across the beam, in other words, the field can be both discrete and continuous.

Assume that the beam field at the medium exit at $z = z_1$ may be defined as

$$A(\xi, \eta, z_1, t) = A_1(\xi, \eta, t)\exp[\mathrm{i}\varphi_1(\xi, \eta, t)], \quad (1)$$

where the amplitude $A_1(\xi, \eta)$ and phase $\varphi_1(\xi, \eta)$ of the wave field, depending on the refraction condition, are determined by solving the transport or parabolic equations for an inhomogeneous medium [9]. If the length of the inhomogeneity region is relatively small and the volume effects in the medium are not taken into account, in the phase screen approach

$$A(\xi, \eta, z_1, t) = A_0(\xi, \eta)\exp[\mathrm{i}kz_1 n(\xi, \eta, t)]. \quad (2)$$

The time t is considered as a parameter and taken into account only in the final result when substituting the given dependences $n(\xi, \eta, t)$, where ξ and η are the coordinates at the medium interface in the plane $z = z_1$. At the observation point with coordinates x, y, z, the wave field $A(x, y, z)$ of the beam propagating in the free space can be obtained as a solution of the parabolic equation

$$2\mathrm{i}k\frac{\partial A}{\partial z} + \frac{\partial^2 A}{\partial x^2} + \frac{\partial^2 A}{\partial y^2} = 0 \quad (3)$$

with the boundary condition defined by (1).

Let us represent the solution of (3) in the form

$$A(x, y, z) = \frac{1}{\mathrm{i}\lambda(z - z_1)}\int_{-W_1}^{W_1}\int_{-W_2}^{W_2} A_1(\xi, \eta) \times \exp\left[\mathrm{i}\varphi_1(\xi, \eta) + \mathrm{i}k\frac{(x - \xi)^2 + (y - \eta)^2}{2(z - z_1)}\right]\mathrm{d}\xi\mathrm{d}\eta, \quad (4)$$

where W_1 and W_2 are the effective beam sizes at the medium exit in the plane $z = z_1$ along the axes ξ and η, respectively. Usually, in studying nonstationary inhomogeneities, the beam size is comparable with the characteristic cross section of the inhomogeneity, or exceeds it.

Obviously, if the transverse gradient of the refractive index is large enough, the function $A_1(\xi, \eta)\exp[\mathrm{i}\varphi_1(\xi, \eta)]$ is fast-changing and cannot be brought out of the integral, as is usually done in the region where the geometrical optics approximation is valid. Therefore, direct integration in (4) for sufficiently large values of W_1 and W_2 faces the problems associated with the need for substantial computing resources, which actually impedes solving the inverse reconstruction problem of inhomogeneity parameters. In terms of geometrical optics, this situation is equivalent to a strong deflection of rays at the medium exit, formation of caustics and multipath areas. Herewith, the deflection angles of rays may be considerably different at the points of the inhomogeneity cross section perpendicular to the direction of propagation of probe radiation. These phenomena indicate the presence of significant refraction which actually violates the beam structure.

Nevertheless, the use of asymptotic methods and vivid physical representations can greatly simplify the procedure of calculating the field $A(x, y, z)$, with preservation of the information content of its wave description (4). Let us find the points of the stationary phase by equating to zero the partial derivatives with respect to ξ and η of the exponent in (4):

$$\xi + \frac{z - z_1}{k}\frac{\partial\varphi_1(\xi, \eta)}{\partial\xi} = x,$$
$$\eta + \frac{z - z_1}{k}\frac{\partial\varphi_1(\xi, \eta)}{\partial\eta} = y. \quad (5)$$

The points of the stationary phase with the coordinates $\xi_m(x, y)$ and $\eta_m(x, y)$ are the solution of the system of equations (5) for the given coordinates x and y of the observation point. The integer index $m \leqslant M$, where M is the number of the solutions of system (5), which is equal to the number of geometrical optics rays arriving at a given observation point. Several such rays may exist in the multipath region. The values $\xi_m(x, y)$ and $\eta_m(x, y)$ in the plane $z = z_1$ correspond to the coordinates of the exit points of these rays from the medium. If system (5) has no solution, this means that there are no rays arriving at a given observation point.

Returning to representation (4) of the field $A(x, y, z)$, we can write it in the form

$$A(x,y,z)=\frac{1}{i\lambda(z-z_1)}\sum_{m=1}^{M}\int_{\xi_m(x,y)-\Delta_\xi}^{\xi_m(x,y)+\Delta_\xi}\int_{\eta_m(x,y)-\Delta_\eta}^{\eta_m(x,y)+\Delta_\eta}A_1(\xi,\eta)$$
$$\times\exp\left[ik\frac{(x-\xi)^2+(y-\eta)^2}{2(z-z_1)}+i\varphi_1(\xi,\eta)\right]d\xi d\eta, \qquad (6)$$

where the values Δ_ξ and Δ_η are selected from the condition that the phase change of the integrand in the predetermined area of integration does not exceed a certain value $\Delta\varphi$ defined by the required accuracy of $A(x,y,z)$ calculation. Thus, instead of integrating over the entire beam section, we may restrict ourselves to the integration over the region that gives the main contribution to the sought-for field and corresponds to the first few Fresnel zones in the vicinity of the exit point of each beam, i.e. in the vicinity of the stationary points with the coordinates ξ_m and η_m.

It is known [9] that such a restriction of the integration area entails a certain error in the calculation of the field $A(x,y,z)$, usually not exceeding a value of ten percent. However, in contrast to the traditional asymptotics of geometric optics that assumes transition to the infinite limits of integration, the field representations near the caustics and in the multipath region, as well as other advantages of wave description, preserve their correctness. Thus, expression (6) provides a unified representation for the field in the observation plane, the integration region localisation near the points ξ_m, η_m being a function of the observation point, which can be determined analytically from equation (5) and depends on the type of the inhomogeneity rather than on the particular type of the beam.

The essential requirement that must be met in finding the field (6) is that the integration regions corresponding to different stationary phase points (at various m) should not overlap [5], and each time this should be checked directly in the calculation of the fields for the beams with a continuously changing intensity. In the case of beams with discrete modulation of the cross-sectional intensity, this requirement is virtually always satisfied, since the regions with a nonzero intensity are sufficiently separated. For such beams, the dimensions Δ_ξ and Δ_η of the integration regions in the vicinity of the stationary phase point should be chosen based on the characteristic dimensions δ_j of the beam's discrete element, such, as for example, the effective width of the ring in Fig. 1a. In this case, the field calculation error caused by the integration region restriction is significantly reduced, since the original field values at the integration region boundary are actually equal to zero. Figure 2 compares the dependences of the field intensity $|A(x)|^2$ in a vicinity of the caustic that arises in passing of the radiation through a focusing layer with a refractive index $n(x)=n_0+\Delta n\exp(-x^2/a^2)$, calculated on the basis of the exact solution (4) and asymptotic representation (6) with $n_0=1.33$, $\Delta n=0.002$, $a=2$ mm.

For a beam element with a discrete structure (Fig. 2a), with the effective element size $\delta_j=0.3$ mm and integration region dimensions $\Delta_\xi=\Delta_\eta=0.3$ mm, these dependences virtually coincide (Fig. 2b). For a circular Gaussian beam with an effective diameter of 2 mm (Fig. 2c illustrates the beam focusing in the caustic region), the exact and asymptotic solutions (Fig. 2d) are expectedly different, the restriction of the integration domain to several Fresnel zones leading to the oscillations of curve (*2*). Note that the use of the traditional asymptotics of geometric optics that assumes transition to the infinite integration limits in (4) causes the appearance of peculiarities in the region of extremum in the dependences

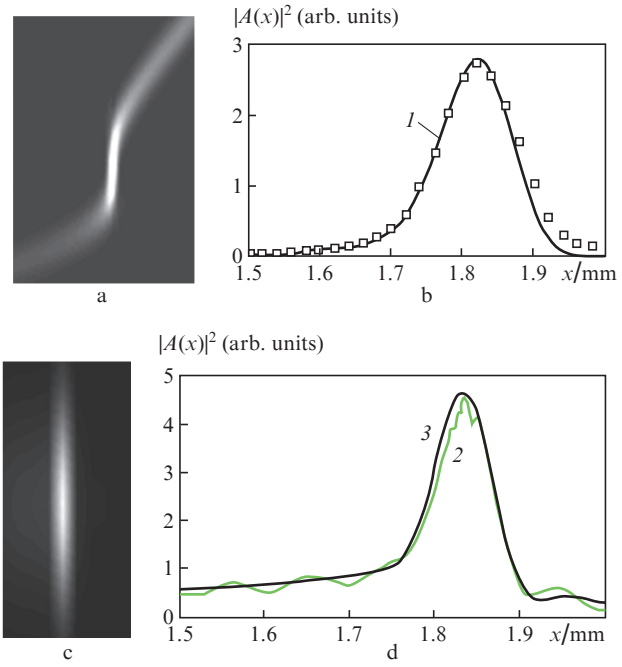

Figure 2. Field intensity distribution in the vicinity of (a, c) the caustic and (b, d) their sections $|A(x)|^2$ calculated on the basis of the asymptotic (□, *1*) and precision (*1*, *3*) solutions for (a, b) a beam with a discrete structure and (c, d) a Gaussian beam.

shown in Figs 2c and 2d – the intensity in that region tends to infinity.

The above results suggest that the resulting representation (6) is optimally adapted to the calculation of the refractive wave field of the discrete-modulated beams and, at the same time, with a controlled accuracy, can be used to calculate the field of the direct-shadow images in the case of beams with a continuous change in intensity.

Figure 3 presents the results of calculation of the refractive images of the cross sections of the beam with a discrete change in intensity, based on the wave representation (6) at $\lambda=0.6328$ μm. The calculations are performed for the typical inhomogeneities of the refractive index, arising in a liquid medium in the presence of density and temperature stratifications.

Figure 3a shows a section of the beam with annular structure at $\delta_j=0.25$ mm (Fig. 1a), which has passed through a diffusion liquid layer with the characteristic thickness $a(x)=a=3$ mm, length $z_1=30$ mm and refractive index

$$n(y,x)=\frac{n_1+n_2}{2}+\frac{n_1-n_2}{2}\tanh\left[\frac{y-y_c(x)}{a(x)}\right], \qquad (7)$$

where $n_1=1.332$ is the refractive index of a less dense (upper) liquid; $n_2=1.337$ is the refractive index of a more dense (lower) liquid; and $y_c(x)$ is the position of the layer centre. The spacing between the rings is $\Delta W=2.5$ mm, the position of the layer centre relative to the beam centre is $y_c=-8$ mm, and the observation plane is located at a distance $z-z_1=600$ mm. In this case, a 'three-path' zone exists between two caustic branches; this determines the possibility of intersection in a small region of three structural beam elements and relevant wave field interference. The caustic branches in the cross section are visualised as a geometric locus of local extremum (turning points) of the beam elements. The calculated image

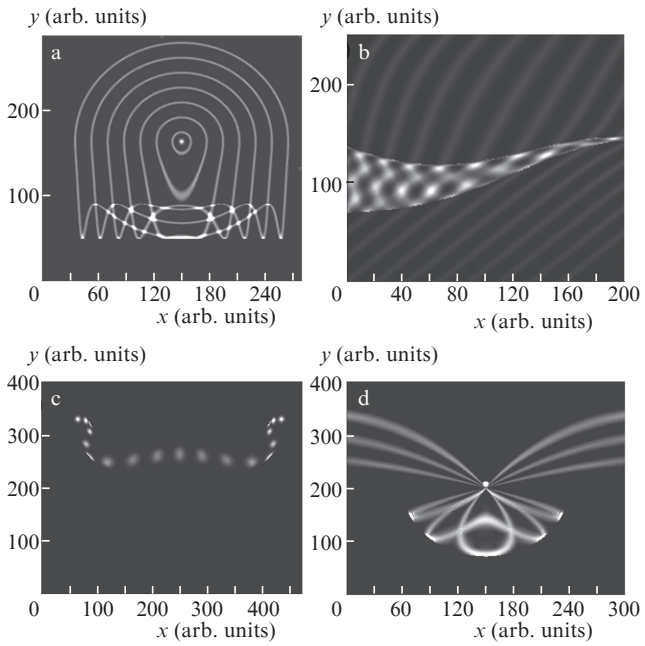

Figure 3. Calculated refractive images of the beams with discrete intensity modulation for typical stratifications in a liquid: (a) diffusion layer (annular beam), (b) wave perturbation in the density stratification (lined tilted beam), (c) cylindrical temperature layer near the heated body (point-like beam) and (d) cylindrical thermal layer near the cooled body (lined horizontal beam).

in Fig. 3 is fully consistent with the experimental image in Fig. 1, obtained with the layer parameters similar to those indicated above.

Figure 3b shows the images of the beam cross sections, the structural elements of which at the entrance to the inhomogeneity region represent parallel segments. In this case, the wave field intensity can be defined as

$$I(r) = \sum_{j=1}^{J} I_j \exp\left\{-\frac{[x-\alpha(y-j\Delta W)]^2}{w_1^2} - \frac{[\alpha x+(y-j\Delta W)]^2}{w_2^2}\right\} \tag{8}$$

and corresponds to a set of elementary beams with elliptical cross section (w_1 and w_2 are the ellipse semi-axes), which at $w_1 \ll w_2$ are visualised as segments. The values ΔW and α define, accordingly, the spacing and slope of the structural elements. Figure 3b demonstrates the refraction of such a beam on a two-dimensional inhomogeneity of the refractive index, arising in propagation of a wave perturbation in the diffusion layer of a liquid [10, 11]. In this case, the position y_c of the layer centre and the layer characteristic size a in relation (7) represent the functions of coordinates and time. Figure 3b visualises the 'three-path' region restricted by the projections of the caustic surface, the distance between which is mainly determined by the gradient $\partial n(x,y)/\partial y$, the parameter $a(x,t)$ varies within 2–6 mm. The results of experimental data relevant to this situation are presented below.

The calculated refraction images relevant to the case of cylindrical temperature stratifications, which may be experimentally implemented as the boundary layers near the heated and cooled objects in water, are shown in Figs 3c and 3d, respectively. The temperature difference at the layer boundary constitutes several tens of degrees, the characteristic dimension of the layer is $a \approx 1$ mm, and the characteristic size of the beam element is $\delta_j = 0.2$ mm. In the experiment, similar images, obtained using the beams with a point-like structure, have been observed in the optical studies on temperature gradients arising in the conditions of the Benard–Marangoni convection [12, 13].

Thus, analysis of expression (6) indicates that, if the condition $\delta_j \ll a$ is satisfied, the wave field of the discretely modulated beams, even in the presence of caustics, has a rather simple structure in the localisation region of the beam element, which is characterised by the intensity dependence on coordinate, similar to that shown in Fig. 2b. This is equivalent to preservation of the character of the image, the informative parameters of which, as applied to solving the inverse problem of refraction, can be the position of caustics and displacements of elements, which depend mainly on the refractive index gradient. If $\delta_j \approx a$, in the case of significant magnitudes of the second derivatives, a 'blurring' of the image is observed (see, as example, Fig. 3c), which requires more detailed analysis of the wave field intensity dependence on coordinates in the reconstruction of inhomogeneities. Quantitative reconstruction of the physical characteristics of the fields in the medium under examination can be based on the analytical approaches to the solution of the inverse problem of refraction and also on numerical algorithms in the framework of the methods of minimising the objective function and correlation analysis using the reference images calculated by means of equation (6).

3. Results of reconstruction of quantitative characteristics of phase objects

In the laboratory experiments described below [11], aimed at visualisation and quantitative diagnostics of the dynamic density inhomogeneities in a liquid (Fig. 4), we used the refractive images obtained in the beams with continuous and discrete intensity variations.

The object of study represents internal waves in a salt-stratified liquid, in which a required density distribution is obtained by changing the NaCl concentration. In this experiment, a certain difference in the levels of transition layers of the liquid is established in the main part of the cuvette and the sluice chamber. The initial perturbation is created in the transition layer (7) between fresh and salt (the density $\rho_2 = 1030$ kg m^{-3}) water by pulling out the sluice chamber's damper (Fig. 4a). The transformation nature of this initial perturbation is well-studied for the Korteweg–de Vries equation [14] and, as the results obtained in this experiment show, the 'rectangular step' splits into a group of nonlinear waves moving from the sluice chamber along the boundary of liquids in the main of part of the cuvette (Fig. 4b). However, as shown in [15], a detailed comparison of the experimental data and theoretical conclusions relevant to propagation of such perturbations requires measuring the density gradient in the dynamic transition layer, which is virtually impossible to implement by means of the contact sensors. Using the beams with discrete intensity modulation (8) enables studying the changes in the effective width of this layer and density gradient immediately after the initial perturbation has occurred. Quantitative diagnostics is accomplished by means of correlation processing of the images obtained using a semiconductor laser module with a wavelength of 550 nm and a power of 3 mW. The structure of the image of the multipath region in a defocused beam in Fig. 4a corresponds to the calculated image in Fig. 3b, which allows the use of a parametric model of the layer (7) to deter-

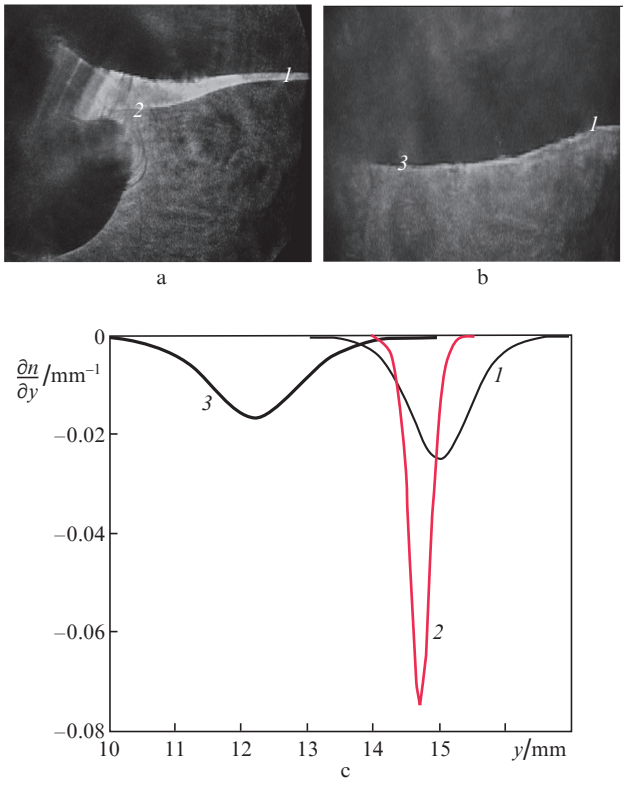

Figure 4. (a, b) Visualisation and (c) quantitative diagnostics of the wave perturbations in a stratified liquid. The characteristic size of the layer a = (*1*) 6, (*2*) 2 and (*3*) 9 mm.

mine the refractive index gradient (or the liquid density). The dependences on the coordinate of the refractive index gradient in the layer are shown in Fig. 4c for the equilibrium position of the layer [curve (*1*)], in the vicinity of a singularity [curve (*2*)], and at the lower point of the wave perturbation [curve (*3*)].

Figure 5 shows the results of a study on the dynamics of the temperature boundary layer [2] that arises near the flat bottom of a metal cylinder with a diameter of 34.5 mm, immersed in water at the temperature of 20 °C, as a result of an abrupt change in the cylinder temperature in the course of rapid filling of the cylinder with water having the temperature of 90 °C. For probing the layer, a He–Ne laser with a power of 1 mW and a wavelength of 0.6328 μm has been used, the characteristic size of the beam element in the direction perpendicular to the cylinder bottom constitutes 0.4 mm. In the experiment, the images of the 'point-like' beam elements, similar to those shown in Fig. 3c, have been obtained.

The peculiarity of the situation is that during the first few seconds after filling the cylinder with hot water the boundary layer thickness is comparable with the characteristic size of the beam element. In this case, we observe a significant 'blurring' of the elements, which does not allow one to study in details the area near the body's boundary surface using the geometric parameters of the images. The time dependence of the temperature gradient (at the distance y = 0.5 mm from the surface) and its derivative in the direction perpendicular to the layer are reconstructed on the basis of the analysis of the intensity distribution (Fig. 2) over the cross section of the beam element. As follows from Fig. 5, during the first few seconds after an abrupt change in the boundary conditions on the surface, an outrunning increase in the second derivative

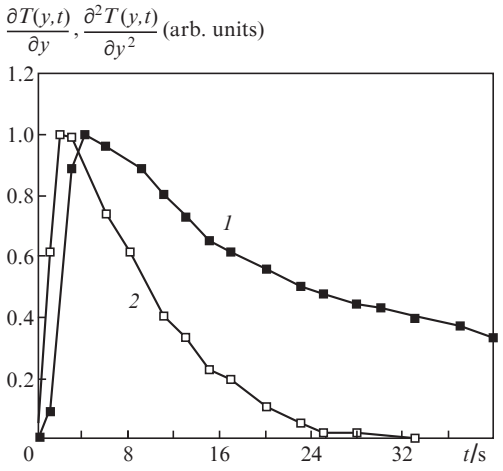

Figure 5. Time dependences of (*1*) the first and (*2*) second temperature derivatives in the direction perpendicular to the cylinder bottom at an abrupt change in its temperature.

$\partial^2 T(y,t)/\partial y^2$ of temperature occurs, and only after that the gradient $\partial T(y,t)/\partial y$ starts to increase. The absolute maximum value of the temperature gradient at the given distance is 53 °C mm^{-1}. If the distance from the surface grows, the gradient reaches its maximum somewhat later, and its value decreases. This fact indicates the formation of a decaying temperature wave in the boundary layer, resulted from an abrupt perturbation on its boundary.

Another possible application of relation (6) is the study of acoustic fields in liquids by means of laser methods [16], in particular, the detection of the spatial domain and the time of occurrence of the ultrasound cavitation by analysing the temporal spectrum $A(x, y, z_1, t)$ containing certain characteristic components of the acoustic field spectrum, which appear in the presence of cavitation. In addition, the refractive images of the discretely-modulated beams are of interest in studying the quantitative characteristics of propagation of ultrasonic waves resulted from the pulse action at the interface of immiscible liquids [17].

4. Conclusions

Thus, relation (6) obtained to describe the wave fields of discretely modulated laser beams in their refraction in phase objects reflects main features of the fields under consideration and allows vivid interpretation of the results of experiments conducted for visualising and studying the extended phase objects in a liquid and carrying out the quantitative analysis of those objects. The wave approach allows the use of complementary information about the intensity distribution and location of caustics in the refracted image, which expands the capabilities of diagnostics of the dynamic objects. Reconstruction of the parameters of the physical processes resulting in a change in the refractive index enables detection of the effects arising in a liquid in the process of changing its characteristics. In particular, the approach outlined in this work is adapted for the analysis of nonstationary processes in liquids, which occurs as a result of the abrupt perturbation of the liquid parameters.

Acknowledgements. This work was supported by the Russian Foundation of Basic Research (Grant No. 14-08-00948a).

References

1. Soifer V.A. (Ed.) *Difraktsionnaya komp'yuternaya optika* (Diffraction Computer Optics) (Moscow: Fizmatlit, 2007).
2. Evtikhieva O.A., Raskovskaya I.L., Rinkevichyus B.S. *Lasernaya refraktographiya* (Laser Refractography) (Moscow: Fizmatlit, 2008).
3. Sarantos C.H., Heebner J.E. *Opt. Lett*., **35**, 1389 (2010).
4. Rinkevichyus B.S., Raskovskaya I.L., Tolkachev A.V. *Proc. 15 th Int. Symp. on Flow Visualization* (Minsk, 2012).
5. Kravtsov Yu.A., Orlov Yu.I. *Geometricheskaya optika neodnoronykh sred* (Geometrical Optics of Inhomogeneous Media) (Moscow: Nauka, 1980).
6. Raskovskaya I.L., Rinkevichyus B.S., Tolkachev A.V. *Kvantovaya Elektron.*, **37**, 1176 (2007) [*Quantum Electron*., **37**, 1176 (2007)].
7. Raskovskaya I.L. *Kvantovaya Elektron.*, **43**, 554 (2013) [*Quantum Electron*., **43**, 554 (2013)].
8. Raskovskaya I.L. *Radiotekh. Elektron*., **54**, 1524 (2009).
9. Vinogradova M.B., Rudenko O.V., Sukhorukov A.P. *Teoriya Voln* (Wave Theory) (Moscow: Nauka, 1979).
10. Bukreev V.I., Gavrilov N.V. *Zh. Prikl. Mat. Mat. Fiz.*, **5**, 51 (1983).
11. Yesin M. et al. *Trudy XI Mezd. Nauchno-Nekhn. Konf. 'Opticheskie metody issledovaniya potokov' (Proceedings of XI Intern. Conf. 'Optical Methods of Stream Research')* (Moscow: MPEI, 2011).
12. Dauby P.C., Desaive T., Bragard J., Cerisier P. *Phys. Rev. E*, **64**, 6301 (2001).
13. Cerisier P., Sylvain J., Dauby P. *Exp. Fluids*, **33**, 391 (2002).
14. Gurevich A.V., Pitaevskiy L.P. *Zh. Eksp. Teor. Fiz*., **65**, 590 (1973).
15. Ostrovskiy L.A., Stepanyants Yu.I. *Izv. Akad. Nauk SSSR, Ser. Mekh. Zidk. Gaza*, **4**, 63 (1982).
16. Grechikhin V.A., Raskovskaya I.L., Rinkevichyus B.S., Tolkachev A.V. *Kvantovaya Elektron*., **33**, 742 (2003) [*Quantum Electron*., **33**, 742 (2003)].
17. Brysev A.P., Yurov V.Y. *Pis'ma Zh. Eksp. Teor. Fiz*., **99**, 94 (2014).